POAC'23
Glasgow, United Kingdom

Proceedings of the 27th International Conference on
Port and Ocean Engineering under Arctic Conditions
12-16 June 2023, Glasgow, United Kingdom

Ice resistance prediction of ships in brash ice channels based on CFD-DEM method

Zhaochun Liu[1], Yong Yin[1], Xiufeng Zhang[1]
[1] Dalian Maritime University, Dalian, China

ABSTRACT

Ships are affected by the disturbance of brash ice when navigating in the brash ice channel. Therefore, this paper investigates the trend of ice-floe resistance under the mutual coupling of ship-ice in a brash ice channel. Firstly, the CFD-DEM coupling numerical method is applied to simulate the ice-water-ship interaction of an ice-area bulk carrier in the brash ice channel. On this basis, in combination with the discrete element method, the motion of brash ice is explained; and then the simulations are conducted to verify the ice resistance, which validates that the numerical model can well simulate the phenomenon and process of ship-ice interaction and can accurately predict the ship's resistance to brash ice. Finally, multiple simulations are carried out to investigate the influence of velocity, ice thickness, and ice concentration on ship resistance, which can provide a reasonable reference for the forecast of ship resistance in the brash ice channel.

KEY WORDS: Brash ice channels; Ice resistance; CFD-DEM; Resistance prediction.

INTRODUCTION

With the seasonal navigation of the Arctic Seaway and the gradual extension of the navigation time, the problem of Arctic navigation has increasingly attracted attention. The navigation of the Arctic waterway not only brings economic benefits to all countries, but also provides scientific assistance to the Arctic scientific research. Research on ships, which are vital transport vehicles in the Arctic waterway, has become increasingly important. The mechanism of ship-breaking ice interaction during the navigation of ships in ice channels is complex. Therefore, conducting research on predicting the resistance of ships navigating in brash ice channels is of great significance. Regarding the measurement and prediction of the crushed ice load on structures, international scholars commonly use methods such as direct measurement on actual ships and ice basin model testing, and have summarized a series of empirical formulas for estimating crushed ice loads. However, both direct measurement and experimental simulation require a large amount of experimentation, and sea trials in ice area require high costs. With the rapid development of computer technology, numerical methods have been widely applied, and numerous attempts have been made on the numerical

calculation of brash ice loads. Among them, the finite element method (FEM) and the discrete element method (DEM) are widely used. The advantage of FEM is that the deformation of sea ice structures can be better investigated. Kim conducted numerical simulations of ship-ice interaction in a brash ice channel using the finite element method and LS-DYNA software, validating the accuracy of their numerical results through ice tank tests (Kim et al., 2013). Guo also utilized the LS-DYNA method to simulate the process of a ship sailing in brash ice channel, analyzing and evaluating their numerical results based on towing tank experiments (Guo et al., 2016). Zhou used the cohesive element method with the finite element method to model the collision between brash ice and propellers (Zhou et al., 2019). Jeon discovered that finite element method with element erosion technology can accurately predict local ice loads, after which they proposed a fatigue damage calculation method relies solely on the probability distribution of local ice loads (Jeon et al., 2022). The advantage of the discrete element method is that it can simulate sea ice as particles that stick together. The destruction and accumulation effect of brash ice can be accurately simulated by changing the parameters of the interaction forms and forces between the particles. It has significant superiority in simulating the discrete characteristics of sea ice. Prasanna developed a simulation tool for ship navigation through brash ice channel using the discrete element method and compared the results with experimental model tests (Prasanna and Hisette, 2018). Luo investigated ship resistance in brash ice channel using the CFD-DEM coupling numerical method, analyzing the effects of ice-particle shapes and coupling calculation schemes on ship-ice interaction (Luo et al., 2020). Huang utilized an enhanced Discrete Element Method to model pre-sawn ice pieces and simulated ship navigation through the pre-sawn ice channel. Results indicating that this method can reasonably estimate the resistance and motion of pre-sawn ice around the ship (Huang et al, 2022). Accurately predicting ice resistance has always been a challenge for safe navigation of ships, so further necessary work is required in related numerical methods.

In this paper, a coupled ship-ice-water model is established by CFD-DEM method to conduct numerical simulation of the interaction process between the ship and the brash ice in the brash ice channel. Firstly, the numerical model setup is introduced and preliminary validation work is conducted by comparing with previous research results. Further quantitative analysis is carried out on factors affecting the brash ice resistance, including ship speed, ice thickness and ice concentration, are quantified and analyzed, providing reference for ship resistance prediction and structural design.

Fundamental Theory

In the coupling process of ship-ice-water, regarding the free surface flow problem of incompressible viscous fluid, the governing equations used throughout the flow field are the continuity equation and the Navier-Stokes equation.

$$\frac{\partial(\rho_f \varepsilon_f)}{\partial t} + \nabla(\rho_f \varepsilon_f \vec{u} \cdot \vec{u}) = -\varepsilon_f \nabla p - \nabla \cdot (\varepsilon_f \overrightarrow{\tau_f}) + \rho_f \varepsilon_f \vec{g} - \overrightarrow{F} \tag{1}$$

The τ_f is found from:

$$\vec{\tau}_f = -u_f(\nabla\vec{u} + (\nabla\vec{u})') + \frac{2}{3}\mu_f(\nabla\vec{u})\ddot{\delta} \tag{2}$$

The $\overrightarrow{F}$ is found from:

$$\overrightarrow{F} = \frac{1}{V_{cell}} \sum_{i=1}^{n_p} \overrightarrow{F_i} = \frac{1}{V_{cell}} \sum_{i=1}^{n_p} (\overrightarrow{F_{di}} + \overrightarrow{F_{bi}} + \overrightarrow{F_{li}} + \overrightarrow{F_{ai}} \overrightarrow{F_{pi}}) \tag{3}$$

The DEM model extends the lagrange formulation to consider the interaction between particles in the particle equation of motion. The contact model of the particles is shown in Figure 1, where particles are combined with each other, and particles of different sizes and shapes are used to form a composite particle of any shape according to the demand.

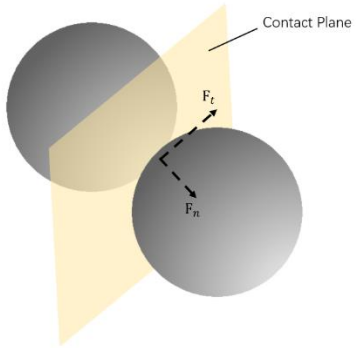

Figure 1. Particle contact model

For the particle contact model, this paper mainly adopts Hertz-Mindlin contact model. The force between two particles can be expressed as:

$$F_{contact} = F_n n + F_t t \tag{4}$$

Where $F_n = -K_n d_n - N_n v_n$, $F_t = \frac{|K_n d_n| C_{fs} d_t}{|d_t|}$. F_n is normal force, F_t is tangential force.

DuBrovin put forward an empirical formula for the resistance of ships under the model scale in the ice breaking test(DuBrovin,1970):

$$\begin{cases} R = C_1 K_A + C_2 K_\varphi F_r n \\ K_A = \frac{1}{4} B^2 \sqrt{C_{conc} h_i} \rho_{ice} (1 + 2\frac{L}{B} f_0 \alpha_H) \\ K_\varphi = C_{conc} h_i B[f_0 + \tan(\alpha_H + \frac{L}{B} \tan(\alpha_0))] \end{cases} \tag{5}$$

Where, R denotes the ice resistance to the model ship; C_1 and C_2 are coefficients, depending on the distribution concentration of brash ice and the width of the channel, respectively; F_r is the Fourier number; n is the power coefficient, depending on the ship type of the model ship; C_{conc} and h_i are the concentration of brash ice and the thickness of brash ice, respectively; f_0 is the friction coefficient, α_0 denote half of the incidence angle of the waterline surface of the model ship and α_H denote the ship forebody diamond coefficient.

Numerical model

A rectangular computational domain is chosen for the numerical simulation of the brash ice channel, with the computational domain in the x-direction in the length direction, the y-

direction in the width direction, and the z-direction in the height direction. As shown in Figure 2.1(a).

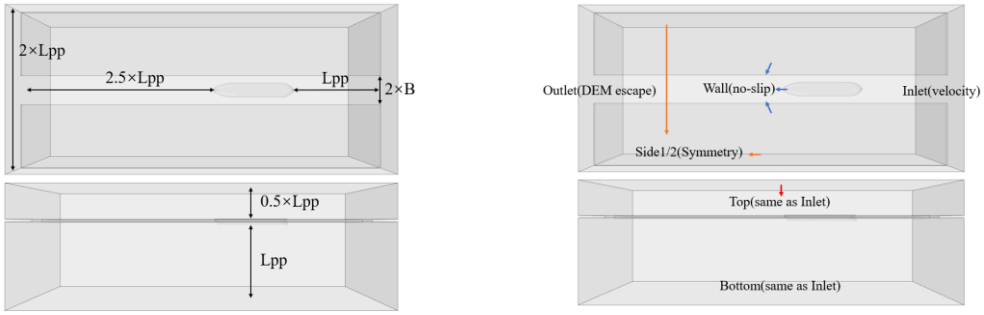

(a) The size of domain (b) Boundary Settings

Figure 2. Computing Domain Setting

The length of the numerical ship model is recorded as Lpp. In order to reduce the calculation time, the calculational domain is set as a rectangular shape with a longitudinal length of 1×Lpp in front of the ship, 2.5×Lpp behind the ship, a width of 2Lpp. Water phase, air phase and brash ice phase are distributed in the calculational domain. The VOF method is used to mark the free water surface, where the air phase is above the free water surface, and the water phase is below, both of which are constant density fluids. Particles of brash ice float on the free water surface.

The velocity inlet (Inlet) is set in the calculation domain: fluid flows into the calculational domain from the inlet, and a specified velocity amplitude is set. The pressure outlet (Outlet) is specified as the working pressure outflow boundary on the entire outlet, ensuring the stability of the domain and allowing the fluid to flow out of the computational domain. At the same time, the brash ice particles that reach the end of the calculational domain are carried out with the fluid flow out of the pressure outlet. The top (Top), bottom (Bottom), the left side (Side1), and the right side (Side2) of the computational domain are all velocity inlets. The boundaries are allowed to fluid inflow with the outside, but do not allow brash ice particles to pass through. The interface of the ship's hull and the layer ice, sides of the ship, are set as the wall (wall). The DEM mode is used to calculate the ship-ice contact force, as shown in Figure 2.1(b).

The model selected in this paper is a Panamanian bulk carrier in brash ice channel. The ship model of the numerical simulation is adopted with a scale ratio of 1:30.682(Luo et al., 2020). The main parameters of the real ship and the ship model are shown in Table 1.

Table 1. Parameters of ship model

Parameters	Full	Model
Scale Ratio	30.682	
Length between perpendiculars (m)	217.00	7.07
Breadth (m)	32.25	1.05
Depth (m)	20.10	0.65
Design draught (m)	12.40	0.40
Design speed in open water (m/s)	7.72	1.39

The brash ice is generated in the numerical brash ice channel by particle jetting. The injector

located around 0.5×Lpp at the bow of the ship. The arrangement of the injector and the direction of the injected brash ice particles as shown. The concentration of brash ice in the channel is controlled by adjusting the spacing of the jet particles, the jet speed and the number of jet particles. In the numerical brash ice channel, the phase to phase interactions are shown as: interaction between DEM particles and DEM particles, interaction between DEM particles and wall, and interaction between DEM particles and VOF phases. As shown in Figure 3. The above model uses the Volume of Fluid (VOF) method to capture the free surface of water and air phases. The flow field around the ship is solved by the CFD method, and the motion and force of the brash ice particles are calculated using the DEM method, with two-way coupling model. The two-way coupling model allows the exchange of mass, momentum, and energy between the particle and the continuous phases. This model enables a more accurate description of the movement of brash ice particles and interaction between ice particles and the flow field.

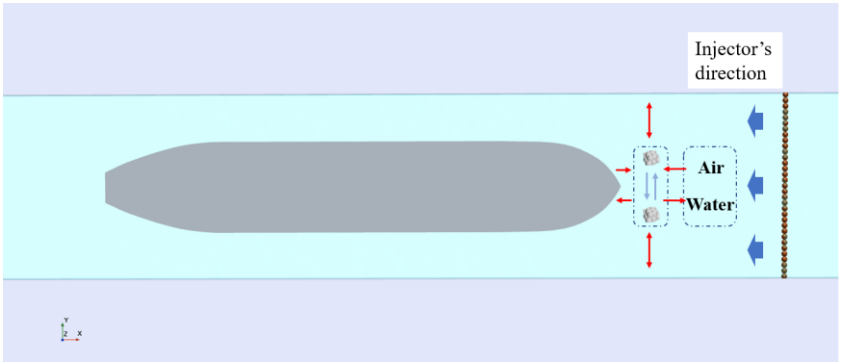

Figure 3. The arrangement of the injector

For the dividing of the grid of the brash ice channel, the key is the coupling effect between the ship, fluid and the brash ice. In this paper, the base size of the grid is selected as 0.2m and sets six layers of prism layers with a growth rate of 1.2 times. The hull of ship part needs a finer grid. The bow and stern parts are encrypted separately. The brash ice floats on the free water surface, the free water surface also needs to be refined. After the grid processing, the total number of grid cells in the computational domain is about 1.5 million.

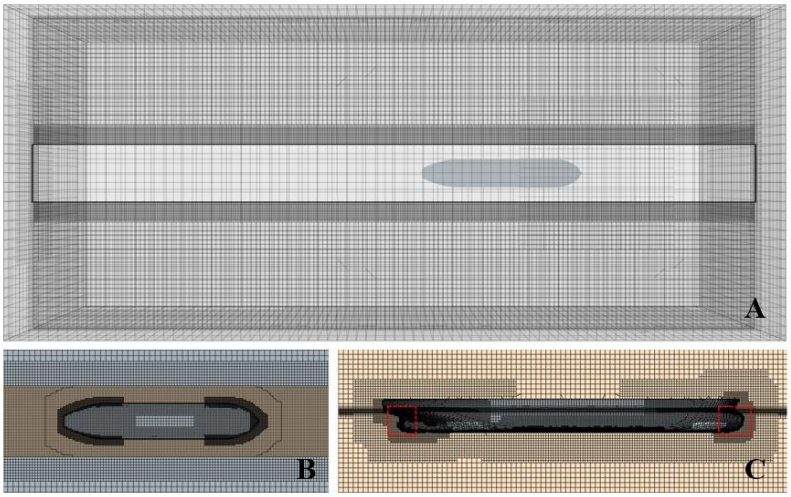

Figure 4. Computational mesh

According to the boundary condition and grid setting in the numerical model, the ship-ice

contact phenomenon when the ship model sails with 0.464m/s is simulated, the concentration of brash ice is about 70%, and the thickness of brash ice is 44.93m is used for the simulation, and the phenomenon during the test with reference to the ice pond is compared with the ship ice action phenomenon in the numerical simulation calculation.

From the Figure 5, it can be seen that the ship-ice contact phenomenon in the numerical simulation is basically the same as in experiments (Hellmann et al., 2005): there is part of the brash ice accumulated in the bow of the ship, part of the brash ice in a flipped state, and part of the brash ice slide along the hull on the side of the ship. When the ship navigates through the brash ice channel, a channel without brash ice slightly narrower than the ship's width is formed behind the ship. As more and more brash ice slide to the back of ship, it gradually converges toward the center of channel under the effect of the wake, finally the channel becomes narrower the farther away from the stern of ship. The simulation results are consistent with the experimental results, indicating that the CFD-DEM method can well simulate the phenomena of ice flipping, accumulation, and sliding when the ship contacts the ice.

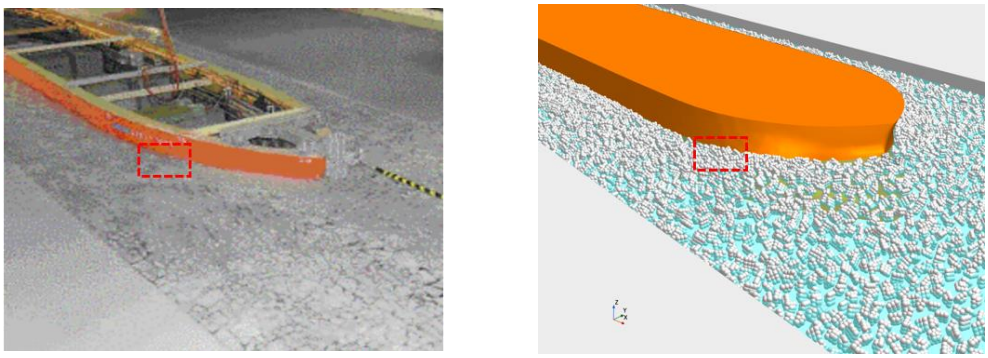

(a) Overturning and accumulation phenomena of brash ice in experimental and numerical simulation

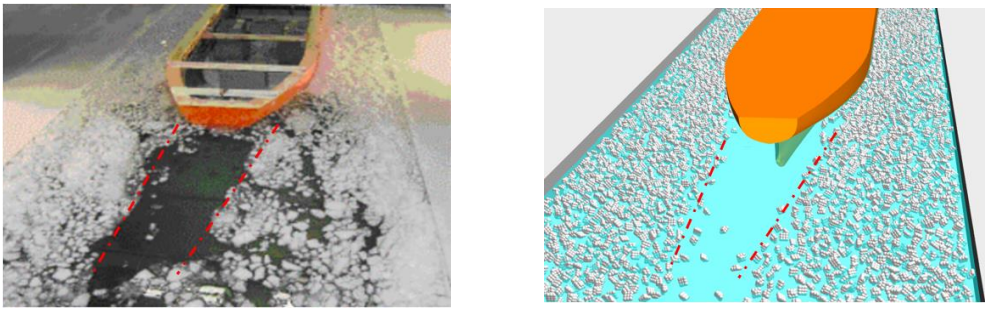

(b) Open water behind the ship in the test and numerical simulation

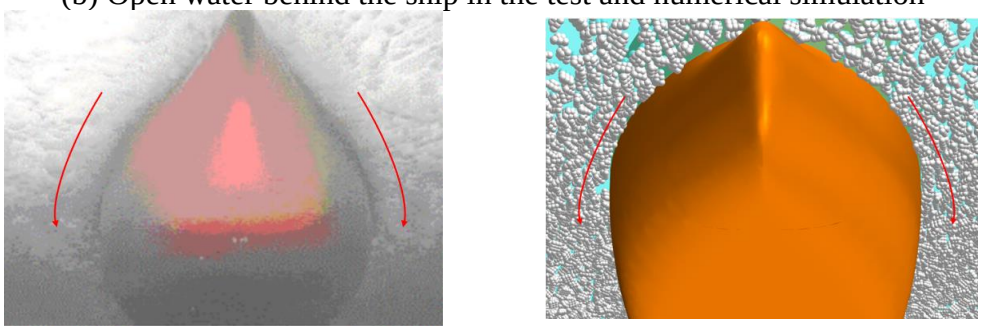

(c) Ice sliding along the hull in experimental and numerical simulations

Figure 5. Comparison of ship-ice contact phenomena

According to the four sets of experimental settings for the corresponding control experiments

of HSVA, the results of resistance simulation calculation are as follows:

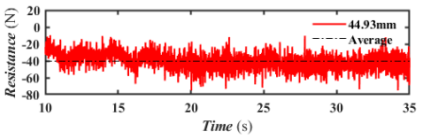

(a) 44.93mm

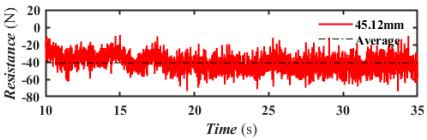

(b) 45.12mm

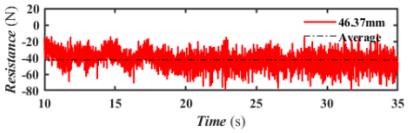

(c) 46.37mm

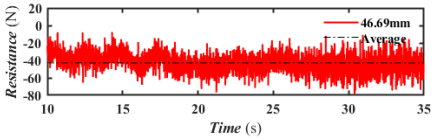

(d) 46.69mm

Figure 6. The resistance curves of ship in brash ice channel

The comparison of numerical model test results and simulation results is shown in Table 2.

Table 2. Comparison of numerical model test results and simulation results

Ice thickness-EFD(mm)	Resistance-EFD(N)	Resistance-CFD(N)	Error(%)
44.93	38.15	40.53	6.23
45.12	40.18	41.00	2.02
46.37	42.72	42.79	0.17
46.69	38.75	42.82	10.50

Numerical results and analysis

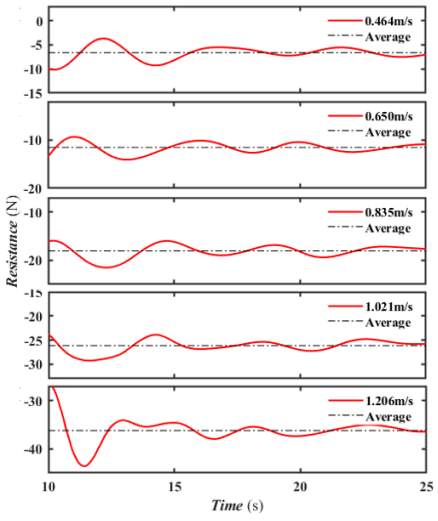

(a) Ice-free channel

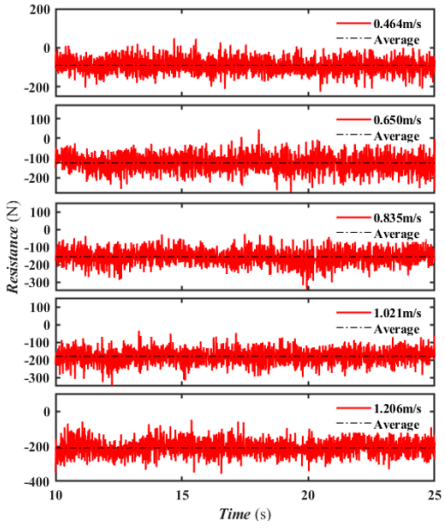

(b) Brash ice channel

Figure 7. Results at different speeds

When a ship navigates in brash ice channel, the speed has a significant impact on the hull resistance of the ship. Figure 7(a) and Figure 7(b) show the time history curves of the ship hull force in ice-free channel and brash ice channel respectively. The concentration of the

brash ice channel is set at 70%, with the thickness of the brash ice set to 65.18mm. Figure 8 shows the average value of resistance with speed. The speed of ship determines the frequency of contact between the ship and the brash ice. From Figure. 8, it can be seen that the ice resistance of the ship gradually increases with the increase of speed. After contacting the brash ice particles, the ship continuously experiences the phenomenon of "collision-sliding-collision", resulting in a sawtooth-shaped fluctuation in the resistance curve during the numerical simulation process. As the speed increases, the time course of the phenomenon "collision-slip-collision" is gradually shortened, and the number of brash ices contacted per unit time increases, resulting in an overall increase in the collision force.

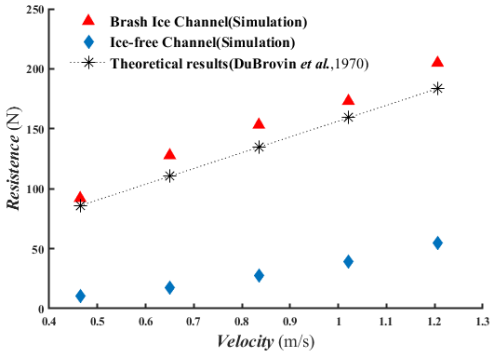

Figure 8. Average value of hull resistance at different speeds

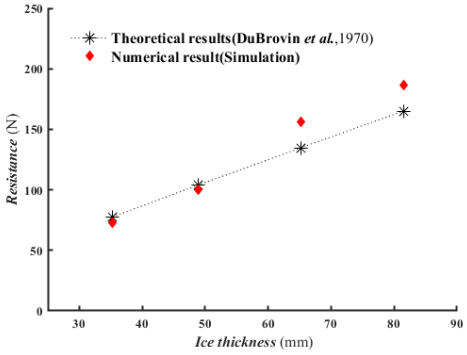

Figure 9. Average value of hull resistance at different ice thicknesses

The thickness of brash ice will have an important impact on the resistance to the ship under the condition of constant speed and concentration during the navigation of the ship in brash ice channel. To investigate the effect of brash ice thickness on the resistance of ice, a simulation was conducted with the ship model velocity of 0.835m/s, the concentration of brash ice of 70%, and the thickness of brash ice of 35.29mm, 48.88mm, 65.18mm, 81.48mm. The simulation result of resistance is shown in Figure 9.

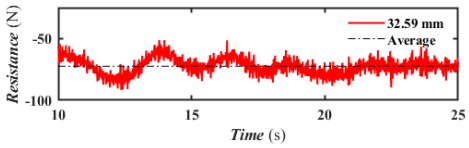

(a) 0.03529m

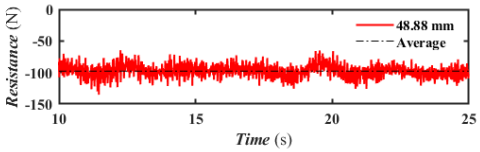

(b) 0.04888m

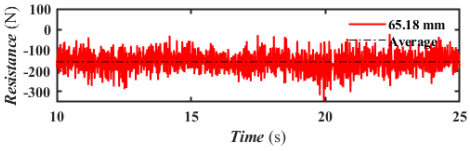

(c) 0.06518m

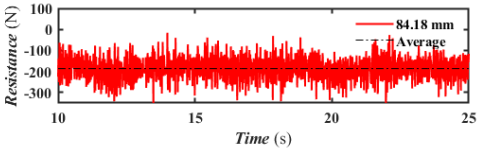

(d) 0.08418m

Figure 10. Results at different ice thicknesses

The relationship between resistance and brash ice thickness was calculated and obtained as shown in Figure 10. The resistance increases with the increase of brash ice thickness. When the ship navigates in the brash ice channel, it will produce certain waves around the ship, and the brash ice plays a certain role in wave dissipation. Under the condition of brash ice thickness is 35.29mm, the peak value of the ship-ice collision force curve is small, and the

water resistance has additional influence on minor thickness of brash ice. With the increase of the brash ice thickness, the more intense interaction of the brash ice on the water flow around the ship. The thicker thickness of brash ice, the heavier the mass of brash ice particles, and the greater the instantaneous force of the ship's hull in contact with the ship ice according to the momentum theorem.

The ship sailing in brash ice channel, the number of brash ices in the channel is random. By using the discrete element method, the concentration of brash ice in the channel can be controlled by controlling the spacing, velocity, and number of ejected particles, as shown in the Figure 11. The thickness of brash ice is 65.18mm, and those particles velocity are set to 0.835m/s. The different spacing of the ejected particles is used to control the concentration of brash ice, and three different ice concentration of 60%, 70% and 80% are selected for the simulation.

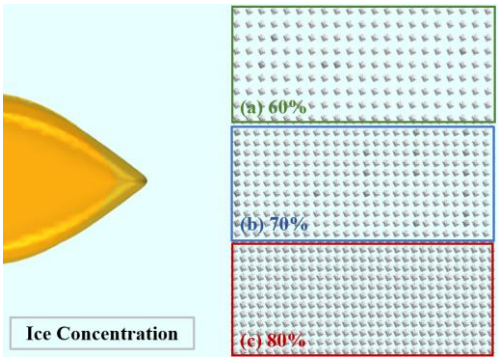

Figure 11. Ice concentration setting

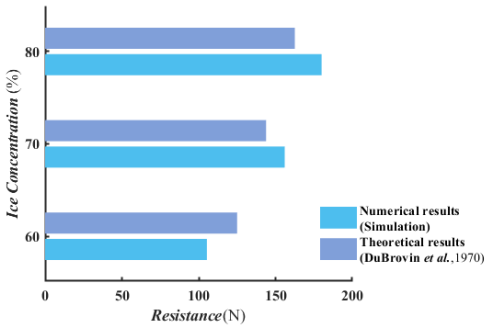

Figure 12. Results at different ice concentration

The simulation results are shown in Figure 12. As concentration of brash ice increases from 60% to 80%, it can be seen that the distribution of brash ice is gradually dense in space. The ice resistance increases with the increase of ice concentration. The greater concentration of the ice is, the greater the probability of contact with the hull, and the greater the number of contact with the hull per unit time. Additionally, the more concentration brash ice is, the more the number of accumulated ice is, and the more the resistance to the hull is.

CONCLUSIONS

In this paper, the CFD-DEM method was used to numerically simulate the ship-ice-water interaction of an ice-area bulk carrier in a brash ice channel. The effects of the speed, ice thickness and the concentration of the brash ice on the hull resistance were investigated. STAR-CCM software was used to simulate the sailing process of ships in the brash ice channel, and the ice resistance and phenomena was compared with the results of experiments. Numerical simulations of ship resistance prediction demonstrate high prediction accuracy, and can reflect typical phenomena of brash ice, such as flipping, accumulation and sliding. These results suggest that the numerical method used for ship-ice-water interaction modeling has certain reference value. By setting the numerical experiments of ship model speed, ice thickness and ice concentration, it was found that the resistance of ship increases with the increase of velocity, which is consistent with the results derived by empirical equations. For the cases of constant speed and concentration, the ship resistance increases with the increase of brash ice thickness. The numerical model is able to reach high accuracy in calculating the ship resistance for smaller thickness. For the variation of the ice concentration encountered by the ship, the higher the concentration of ice, the higher resistance on the ship. This is

explained by the fact that the number of ice particles encountered per unit time increases with increasing concentration.

REFERENCES

DuBrovin, O. V. (1970). *Calculation of broken ice resistance based on model testing.* University of Michigan.

Guo, C. , Li, X. , Wang, S. , & Zhao, D., 2016. A numerical simulation method for resistance prediction of ship in pack ice. *Journal of Harbin Engineering University*.

Hellmann, J. H., Rupp, K. H., & Kuehnlein, W. L., 2005. Model tests in brash ice channels. In *International Conference on Offshore Mechanics and Arctic Engineering*. Vol. 41960, pp. 923-930.

Huang, L., Li, F., Li, M., Khojasteh, D., Luo, Z., & Kujala, P. (2022). An investigation on the speed dependence of ice resistance using an advanced CFD+ DEM approach based on pre-sawn ice tests. *Ocean Engineering*, 264, 112530.

Jeon, S., & Kim, Y. (2022). Fatigue damage estimation of icebreaker ARAON colliding with level ice. *Ocean Engineering*, 257, 111707.

Kim, M. C., Lee, S. K., Lee, W. J., & Wang, J. Y., 2013. Numerical and experimental investigation of the resistance performance of an icebreaking cargo vessel in pack ice conditions. *International Journal of Naval Architecture and Ocean Engineering*, 5(1), pp.116-131.

Luo, W., Jiang, D., Wu, T., Guo, C., Wang, C., Deng, R., & Dai, S., 2020. Numerical simulation of an ice-strengthened bulk carrier in brash ice channel. *Ocean Engineering*, 196, 106830.

Prasanna, M., & Hisette, Q., 2018. Discrete Element Simulation of Ships Navigating Through Brash Ice Channels. In *OTC Arctic Technology Conference*. OnePetro.

Zhou, L., Wang, F., Diao, F., Ding, S., Yu, H., & Zhou, Y.,2019. Simulation of ice-propeller collision with cohesive element method. *Journal of Marine Science and Engineering*, 7(10), 349.